Cell

# Structural Basis for the Histone Chaperone Activity of Asf1

Christine M. English,[1] Melissa W. Adkins,[1] Joshua J. Carson,[1] Mair E.A. Churchill,[2,3,*] and Jessica K. Tyler[1,3,*]
[1] Department of Biochemistry and Molecular Genetics
[2] Department of Pharmacology
School of Medicine, University of Colorado, Aurora, CO 80045, USA
[3] These authors contributed equally to this work.
*Contact: jessica.tyler@uchsc.edu (J.K.T.), mair.churchill@uchsc.edu (M.E.A.C.)
DOI 10.1016/j.cell.2006.08.047

## SUMMARY

Anti-silencing function 1 (Asf1) is a highly conserved chaperone of histones H3/H4 that assembles or disassembles chromatin during transcription, replication, and repair. The structure of the globular domain of Asf1 bound to H3/H4 determined by X-ray crystallography to a resolution of 1.7 Å shows how Asf1 binds the H3/H4 heterodimer, enveloping the C terminus of histone H3 and physically blocking formation of the H3/H4 heterotetramer. Unexpectedly, the C terminus of histone H4 that forms a mini-β sheet with histone H2A in the nucleosome undergoes a major conformational change upon binding to Asf1 and adds a β strand to the Asf1 β sheet sandwich. Interactions with both H3 and H4 were required for Asf1 histone chaperone function in vivo and in vitro. The Asf1-H3/H4 structure suggests a "strand-capture" mechanism whereby the H4 tail acts as a lever to facilitate chromatin disassembly/assembly that may be used ubiquitously by histone chaperones.

## INTRODUCTION

The packaging of the eukaryotic genome into chromatin is essential for normal growth, development, and differentiation. The repeating unit of chromatin is the nucleosome core particle, which comprises 147 bp of DNA wound around a histone octamer (Luger et al., 1997). Chromatin is a dynamic structure that tightly regulates transcription, replication, repair, and recombination. In the context of these processes, the most severe alteration of chromatin structure is the removal of histone proteins from DNA (chromatin disassembly) or the deposition of histone proteins onto naked DNA (chromatin assembly). The ordered packaging of DNA into chromatin is thought to involve the initial deposition of a heterotetramer of histones H3/H4 followed by two heterodimers of histones H2A/H2B to form the nucleosome. This process is mediated by histone-chaperone proteins that regulate the association of the basic histone proteins with the DNA, which permits the nucleosome to form in an ordered and controlled manner (Akey and Luger, 2003; Loyola and Almouzni, 2004).

The histone-chaperone anti-silencing function 1 (Asf1) is the only histone chaperone that is implicated in both replication-dependent and replication-independent chromatin assembly (Nakatani et al., 2004). Asf1 is also a critical factor in multiple other cellular processes. For example, Asf1 is a histone H3/H4 chaperone that assists chromatin assembly factor 1 (CAF-1) during the assembly of newly synthesized DNA into chromatin in vitro (Mello et al., 2002; Smith and Stillman, 1991; Tyler et al., 1999) and is required for replication-independent chromatin assembly together with the Hir histone chaperone (Green et al., 2005; Tagami et al., 2004). Asf1 also mediates chromatin disassembly from promoters in budding yeast during transcriptional activation (Adkins et al., 2004) and chromatin disassembly and reassembly during transcriptional elongation (Schwabish and Struhl, 2006). In fact, all non-DNA bound histones are bound to Asf1 (Groth et al., 2005; Tagami et al., 2004), underscoring its fundamental role as a central histone chaperone in eukaryotes.

The function and structure of Asf1 are highly conserved among eukaryotes. The N-terminal 155 residues of Asf1 form a globular core that consists of an immunoglobulin-like fold (Daganzo et al., 2003; Mousson et al., 2005) with highly conserved acidic patches that are predicted to mediate interactions with histone H3. The structures of histones H3 and H4 have also been determined as components of the nucleosome core particle and histone octamer (Arents et al., 1991; Luger et al., 1997). The yeast and *Xenopus laevis* nucleosome structures underscore the structural and functional conservation of this complex throughout evolution (White et al., 2001). Thus, it is well known how the individual histones interact with each other and with DNA, but there is little information about the interaction of the histones with each other or with chaperones in the absence of DNA. As a result, the mechanisms by which the nucleosomes are assembled and disassembled are not well understood.

Recently, we biophysically characterized the Asf1-H3/H4 complex and demonstrated that Asf1 binds to a heterodimer of histones H3 and H4 (English et al., 2005). In

addition, yeast two-hybrid analysis suggests that the C terminus of histone H3 interacts with Asf1 (Munakata et al., 2000), and NMR chemical-shift mapping revealed interactions of an H3 peptide (residues 122–135) with a highly conserved and acidic patch on the concave surface of Asf1 (Mousson et al., 2005). This histone H3 peptide corresponds to helix 3, which is a crucial part of a four-helix bundle that forms the H3:H3 dimerization interface in the nucleosome (Luger et al., 1997). Furthermore, a disruptive mutation in the middle of this H3-interacting region of Asf1, V94R, abolished the interaction with histone H3 (Mousson et al., 2005). These data raised the possibility that the region that mediates H3:H3 dimerization in the H3/H4 heterotetramer may also be the region of H3 that binds to Asf1.

In this study, we have determined the crystal structure of Asf1 bound to histones H3/H4, revealing how a histone chaperone binds histones and how the structures of H3 and H4 differ outside of the histone octamer. We have confirmed that Asf1 binds to a heterodimer of histones H3/H4 and that Asf1 not only interacts with histone H3 but also with the C-terminal tail of histone H4 in vivo and in vitro. Of interest, the C-terminal tail of H4 undergoes a major conformational change upon binding to Asf1, suggesting a mechanism by which the H4 tail may act as a handle for the assembly and disassembly of the H3/H4 heterotetramers by Asf1.

## RESULTS

### Asf1, H3, and H4 Form a Heterotrimeric Complex

In order to investigate how Asf1 interacts with histones H3 and H4, we determined the structure of the globular core of Asf1 bound to a histone H3/H4 heterodimer at a resolution of 1.7 Å (Figure 1). N-terminal truncation of the histones and coexpression of the three proteins were necessary to obtain the crystals, which contained the conserved region of *Saccharomyces cerevisiae* Asf1 (yAsf1, 1–169) together with *Xenopus laevis* histones H3 (60–135) and H4 (20–102) (Figure 1A). A single Asf1-H3/H4 complex formed the asymmetric unit in the crystals, which belong to space group $P3_121$ (Table S1). The structure was solved by molecular replacement with the structures of Asf1 and the histone H3/H4 dimer from the nucleosome (Figure 1B) (Daganzo et al., 2003; Luger et al., 1997). The final refined model (Table S1) contains yAsf1 (1–164), *Xenopus* H3 (61–134), *Xenopus* H4 (21–101), solvent molecules, and ions.

The overall structure of the Asf1-H3/H4 complex reveals an extensive interaction interface of Asf1 with both histones H3 and H4 (Figure 1B; Table S2). As previously described for the structures of free Asf1 (Daganzo et al., 2003; Mousson et al., 2005), the core of Asf1 is an elongated β sandwich domain with three α helices in the loops between the β strands. This structure has a concave face comprising β strands β3, β4, and β6–9, with high sequence-conservation across species and a distinctly negative charge. In fact, this is the site of histone H3 binding

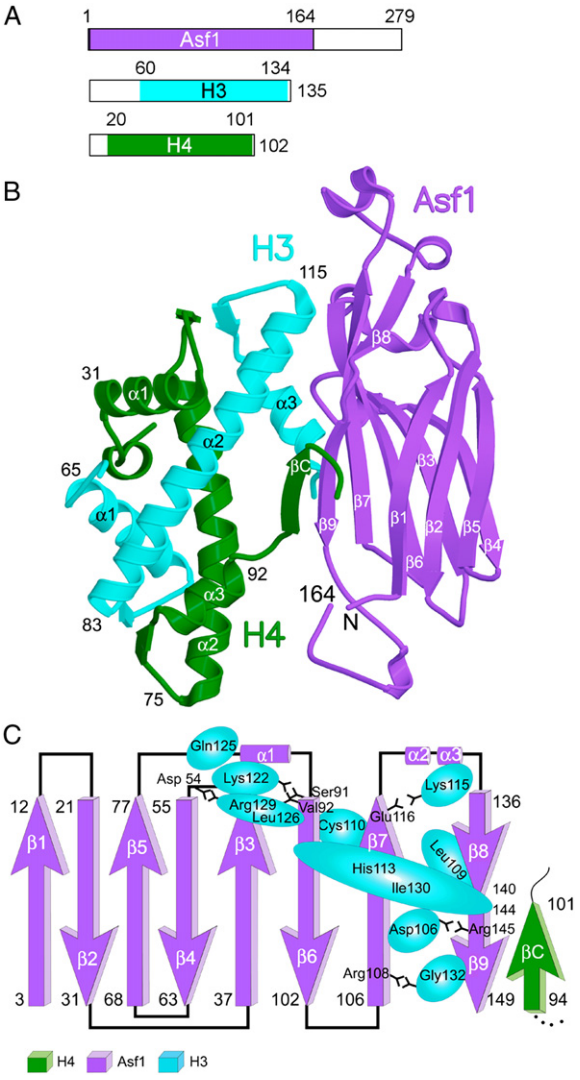


**Figure 1. Asf1-H3/H4 Structure**

(A) Regions of the Asf1, H3 and H4 proteins that appear in this structure are shown as colored regions of the boxes representing the full-length proteins.

(B) The ribbon diagram shows the overall structure of the Asf1-H3/H4 complex, with Asf1 in violet, H3 in cyan, and H4 in green. The major secondary structure elements are labeled.

(C) Topology diagram of Asf1 with contacts between Asf1 and H3 mapped to indicate the extent of H3-Asf1 interactions. The amino acids of histone H3 that significantly contribute to the Asf1 interface are represented by the cyan ovals, whose sizes are proportional to the extent of the buried surface and are labeled accordingly.

(Figures 1C and 2). The contacts between H3 and Asf1 are extensive and result in a buried surface area of 909 $Å^2$. The histones retain the configuration of the conserved histone fold (Luger, 2003) with a few important exceptions. Much of the α-helical region (amino acids [aa] 60–85) of H4 is near, but not in direct contact with, Asf1 (Figure 1C). However, the C terminus of H4 forms a new β strand (H4 βC) with the core of Asf1, which creates a hydrogen

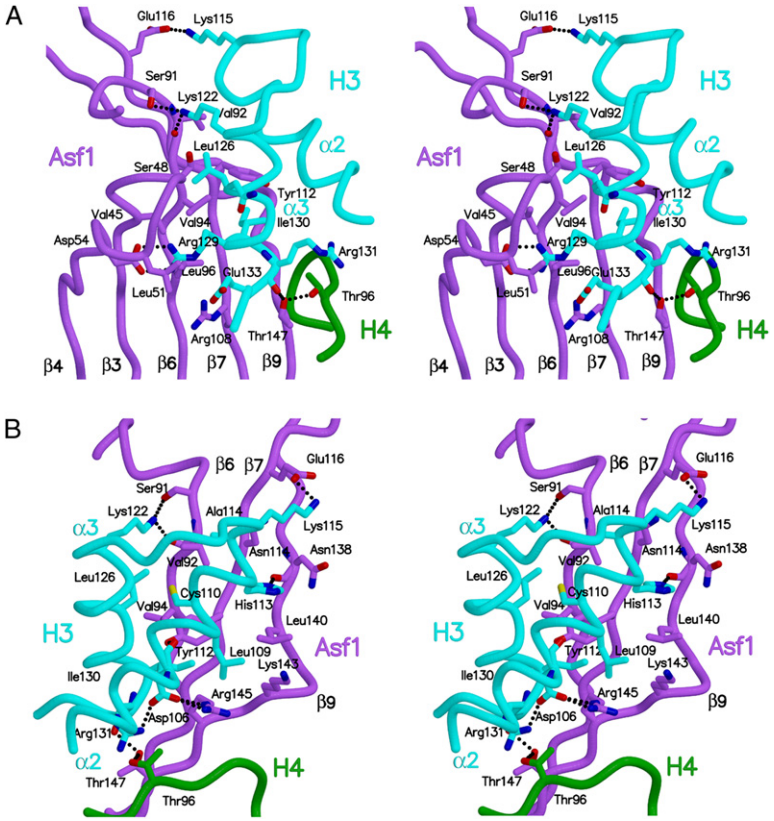


**Figure 2. Interactions of Asf1 with Histone H3**

(A) The stereodiagram shows the details of the interface between Asf1 and H3 focusing on the interactions mediated by alpha helix (α3) of histone H3. Asf1 is colored in violet, H3 in cyan, and H4 in green, with several residues labeled and dotted lines to indicate inferred hydrogen bonds.

(B) The view in this stereodiagram is rotated approximately 120° clockwise about the vertical axis and 25° toward the viewer about the horizontal axis compared to panel (A) to show the details of the interface between Asf1 and alpha helix (α2) of histone H3, colored as in panel (A).

bonding network connecting all three proteins, mediated by T147 of Asf1 (Figure 2). In addition, the H4 C terminus interacts with the core of Asf1 between β1 and β8 and β9, which greatly contributes to the total Asf1-H4 buried surface area of 506 Å$^2$.

## Asf1 Directly Interacts with H3

Analysis of the Asf1-H3 interface reveals that the extensive interaction of histone H3 with Asf1 includes H3 α2 in addition to α3 (Figures 1B and 1C). The region of the Asf1-H3 interface that is mediated by the C-terminal helix of H3 (α3, residues 122–134) makes extensive contacts with each of the Asf1 β strands on the concave face of the protein (Figure 2A). Asf1 V94, which is an important residue for the interaction with histone H3, lies within this region, and it is clear why substituting this residue with an arginine would disrupt H3 binding (Mousson et al., 2005). However, the extent of the contacts between Asf1 and H3 is not limited to α3 of histone H3, as was previously thought, because the C-terminal part of H3 α2 (106–115) and the loop connecting α2-α3 (aa 114–122) interact with residues in β7–9 of Asf1 (Figure 2B). Specifically, there are a number of inferred electrostatic interactions and hydrogen bonds that we would expect to play important roles in the stability of the Asf1-H3 complex, such as $D54_{Asf1}$-$R129_{H3}$, $R145_{Asf1}$-$D106_{H3}$, and $T147_{Asf1}$-$R131_{H3}$ (Figures 2A, 2B, and S1; Table S2). In addition, many van der Waals interactions also contribute to the stabilization of this complex (Table S2).

We conclude that Asf1 and H3 form an extensive interface with a high degree of shape complementarity and specificity due to a large number of specific hydrogen bonds, ion pairs, and van der Waals interactions.

## Asf1 Directly Interacts with H4

It has been widely assumed that the interaction of Asf1 with histones H3 and H4 is mediated solely by the C-terminal helix of histone H3 (Mousson et al., 2005; Munakata et al., 2000), but the Asf1-H3/H4 structure clearly shows that Asf1 also directly binds to histone H4. Figure 3A shows the electron density map of the C-terminal tail of H4, with F100 binding in the hydrophobic core of Asf1, to illustrate the quality of the data in this region. H4 interacts with two separate parts of Asf1. Residues in the histone-fold core of H4, specifically in α2 (Y72 and H75) and α3 (Y88), interact with Y162 in the C-terminal part of Asf1 (Figure 3B). However, these residues are also involved in significant crystal-packing contacts with symmetry-related H3 and H4 molecules, which may influence the details of the structure in this region.

The more extensive and intriguing interaction between Asf1 and histone H4 occurs within the last 10 residues of the H4 protein. H4 residues 95–98 form an additional anti-parallel β strand (βC) with β9 of Asf1 through several main-chain hydrogen bonds (Figures 3B and 3C, Table S2). Within this β strand, $T96_{H4}$ Oγ1 forms a hydrogen bond with $T147_{Asf1}$ Oγ1 that in turn hydrogen bonds

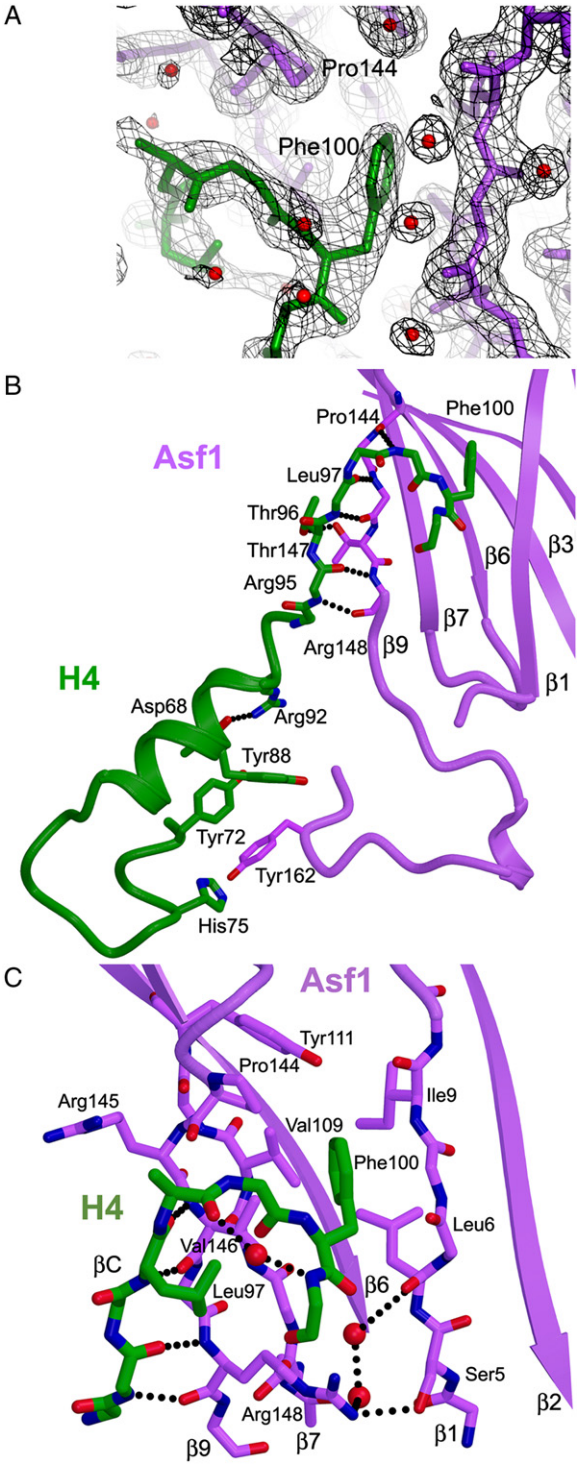


**Figure 3. Interactions of H4 with Asf1**

(A) The electron density map ($\sigma_A$ weighted 2Fo-Fc map contoured at 1 $\sigma$) is shown with Asf1 in violet, solvent molecules in red, and H4 in green.

(B) The diagram illustrates the two regions of H4 that bind to Asf1. The side chains of H4 that interact directly with Asf1 are shown with other portions of the proteins shown in a ribbon representation. The figure is colored as in panel (A), with oxygen atoms in red and nitrogen atoms in blue, and inferred hydrogen bonds are shown as dotted lines.

(C) Close-up view of the H4 C-terminal interaction with the core of Asf1. The view is zoomed in and rotated slightly clockwise about the vertical axis compared to panel (B).

to the main chain of H3, linking all three proteins. In addition, the five final amino acids of H4 interact with Asf1 behind the newly formed β strand, inserting into a hydrophobic pocket created between β strands β1 and β9 (Figure 3C). An important contributor to this interaction is the F100 side chain of H4 (Figures 3A and 3C), which itself buries 172 Å$^2$ of surface area, nearly 35% of the total surface area of the Asf1-H4 interface, through van der Waals interactions with Asf1 L6, V146, Y111, V109, and P144 (Figure 3C). Therefore, H4 significantly contributes to the binding of the H3/H4 dimer to Asf1 through several main-chain and side-chain hydrogen bonds as well as burial of a key hydrophobic residue.

## Structural Changes Occur in the Formation of the Asf1-H3/H4 Complex

Comparison of the Asf1-H3/H4 structure with the structures of free Asf1 reveals subtle conformational changes that occur in Asf1 upon binding to the H3/H4 dimer (Figure 4A). The overall root-mean-square deviation (rmsd) of main-chain atoms of Asf1 in the Asf1-H3/H4 complex compared to the free proteins is 2.42 Å, 1.79 Å, and 1.42 Å for the yAsf1 structure at 2.95 Å resolution (PDB ID 1wg3 [Padmanabhan et al., 2005]), yAsf1 structure at a resolution of 1.5 Å (PDB ID 1roc, [Daganzo et al., 2003]), and hAsf1a structure determined by NMR (PDB ID 1tey [Mousson et al., 2005]), respectively. The largest differences between the structures occur in the loop regions, as expected for structures determined by different methods or crystallized in different space groups. However, the β3-β4 loop moves approximately 6 Å closer to H3 from its position in free Asf1 (PDB ID 1roc), and the strands β3 and β4 move nearly 2 Å away from H3 around residue D54 in β4, which together appear to facilitate the formation of the $D54_{Asf1}$-$R129_{H3}$ ion pair and surrounding contacts. The movements about this pivot point (D54) in β3 and β4 result in an overall less-twisted β sheet and a shift of up to 3.5 Å between β3 and β4 of Asf1 and in the associated loops (Figure 4A). However, this region of Asf1 (aa 35–77) is also involved in crystal-packing contacts with H3 (aa 60–72) and H4 (aa 20–31) of symmetry related molecules so that the significance of these structural differences is difficult to evaluate in the context of this crystal.

The structural changes that take place in Asf1 to accommodate the binding of the H4 C terminus are minor. As seen in Figure 4B, which shows surface representations of Asf1 in the complex compared to free Asf1, very small structural changes occur for insertion of H4 F100 into the core of Asf1 (<0.9 Å), but these result in noticeably better shape complementarity in the complex. Although no significant changes in the backbone conformation in this region of Asf1 occur in the formation of the $\beta C_{H4}$-$\beta 9_{Asf1}$

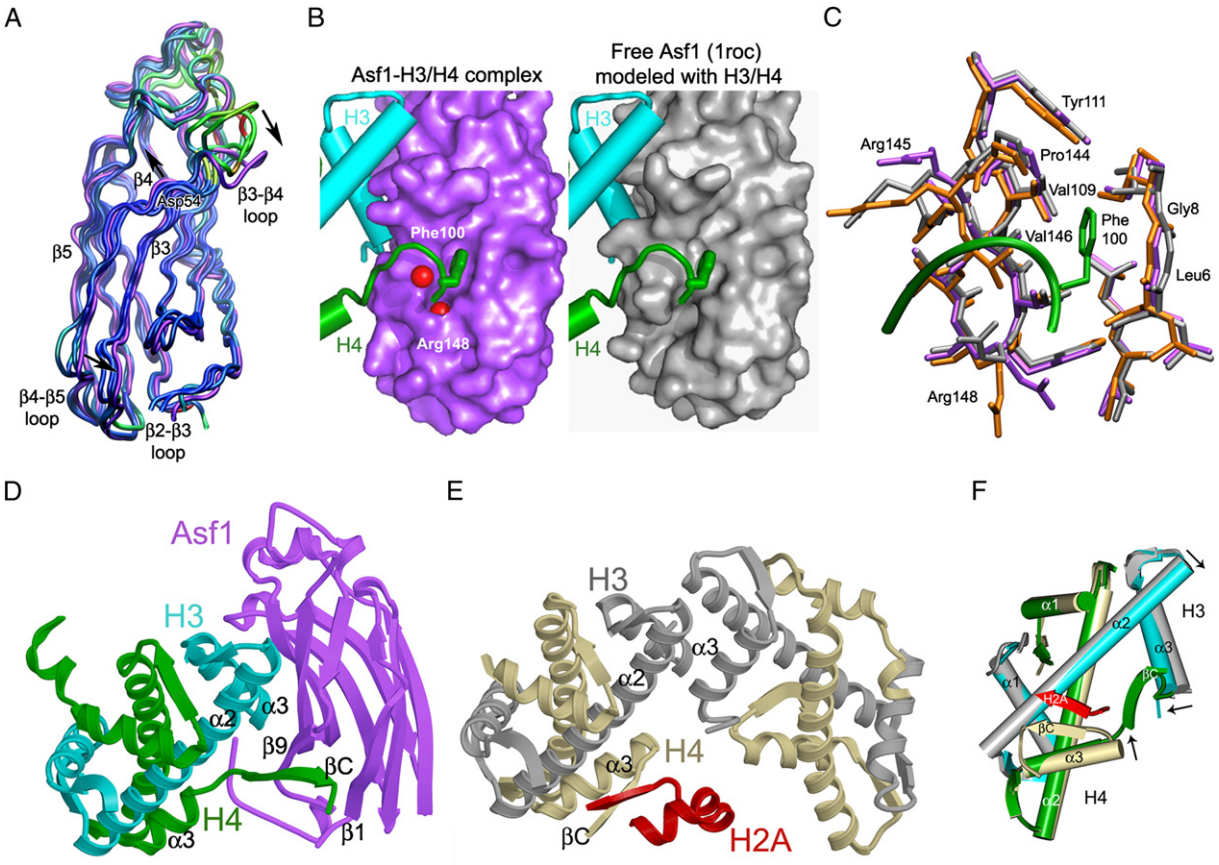


**Figure 4. Asf1 and Histones Undergo Structural Changes to Accommodate Binding**

(A) The overlay diagram of Asf1 from this study (in violet) has the three other Asf1 structures superimposed. The free Asf1 models are colored according to rmsd value from red (most different) to blue (most similar). Arrows indicate the directions and positions of notable structural changes, and Asp54 is indicated.

(B) Surface representations of Asf1 in the current structure on the left and free Asf1 modeled with histones (from PDB 1roc (Daganzo et al. [2003]). H3 is in cyan, H4 is in green, and free Asf1 is in grey. Water molecules are shown as red spheres.

(C) The superimposed Asf1 proteins are from two Asf1 structures (1roc is in grey and 1wg3 is in orange) overlaid onto the Asf1-H3/H4 complex.

(D) Ribbon diagram of the Asf1-H3/H4 complex, with Asf1 colored in violet, H3 in cyan, and H4 in green.

(E) Ribbon diagram showing the histone H3/H4 heterotetramer from the nucleosome core particle (PDB ID 1k5x [Davey et al., 2002]) oriented so that the H3/H4 dimer on the left is superimposed with the H3/H4 dimer in panel (A), with coloring of H3 in silver, H4 in tan, and H2A in red.

(F) Cartoon diagram showing the superposition of the H3/H4 dimer from the Asf1-H3/H4 complex onto one H3/H4 dimer with the C terminus of H2A from the nucleosome, as in panels (A) and (B). Black arrows indicate structural differences between the helices of the histones that occur in the different environments.

anti-parallel β-sheet extension, there are slight side chain movements that facilitate this interaction. For example, R145 rotates 180° about χ1 to create space for the H4 tail to enter the core of Asf1 (Figure 4C), and the side chain of R148 rotates about χ3 to further enclose the binding pocket around F100. Without these subtle changes, H4 F100 would clash with hydrophobic residues that line the cleft of the Asf1 core (Figure 4B). Interestingly, the minor adjustments that would be necessary in Asf1 for H4 binding are suggestive of a lock-and-key binding mechanism, which would be an energetically favorable interaction.

In contrast, there is a profound structural change for histone H4 in the Asf1-H3/H4 complex when compared to the structure of H4 in the nucleosome core particle or histone octamer (Figures 4D–4F). Panel (E) in Figure 4 shows that the C-terminal tail of histone H4 in the nucleosome folds back over α3 of H4 and that residues 96–99 of H4 form a two-stranded parallel β sheet with residues 100–103 of histone H2A. However, in complex with Asf1, α3 in the H4 C terminus terminates one turn earlier than in the nucleosome and extends 180° in the opposite direction so that residues G94–L97 can form the anti-parallel β sheet and insert into the core of Asf1 (Figure 4D). In fact, the rmsd value for the backbone atoms of the H4 protein in the nucleosome (PDB ID 1k5x chain B) compared to the H4 protein in the Asf1-H3/H4 structure is 1.80 Å (Figures 4D–4F). This value is high for two identical proteins and is due solely to the drastic conformational change of the C terminus, with a small portion attributed to deviations at the N terminus. Specifically, the rmsd for the H4

C-terminal tail (aa 92–102) compared to nucleosomal H4 is 3.15 Å, and, without the C-terminal residues, the rmsd is 0.72 Å. Importantly, when superimposed onto the H4 protein in the nucleosome (1kx5), the octamer (1tzy), the nucleosome with H2AZ (1f66), or the nucleosome with macro H2A (1u35), all H4 proteins have the same C-terminal tail structure except for H4 bound to Asf1.

The C terminus of histone H3 in the Asf1-H3/H4 complex has a slightly different structure in comparison to its structure in the nucleosome (Figures 4D–4F). In the nucleosome, α3 of H3 extends to the very end of the protein. However, when bound to Asf1, the last few residues of α3 of H3 unfold so that they do not clash with Asf1. In fact, the rmsd for the overall H3 protein is 0.94 Å, but for the residues in H3 α3 (121–134), the rmsd is higher (1.31 Å). There is also a change in the interhelical angle between α2 and α3, which can be described as a scissoring motion with an approximate decrease in the scissoring angle of 8° for H3 in the Asf1-H3/H4 complex compared with the nucleosome. A smaller scissoring motion is observed for histone H4 (Figure 4F). Thus, the histone fold exhibits some flexibility in α3 of both histones, regions that are important in the structure of the nucleosome.

## Disruption of Asf1 Function by Mutations in the Histone Binding Interface of Asf1

To assess the validity and contribution of the Asf1-H3/H4 interactions revealed by the structure, amino acid substitutions were made in the budding yeast Asf1 protein (Table 1). In order to weaken the interaction between Asf1 and H3, we made substitutions T147E, R145E, Y112A, and S48R in Asf1. The interaction between Asf1 and histone H4 was tested with mutants T147E, V109M, V146L, P144Y, L6M, and Y162A in the core of Asf1 and C-terminal tail (Figure 3). None of these Asf1 mutations significantly affected the expression level of Asf1 (Figure S2, data not shown).

We examined the effects of the single Asf1 mutations on the function of Asf1 in transcription, cell cycle, DNA repair, and replication. The deletion of *ASF1* leads to a slow-growth phenotype (Tyler et al., 1999), which is linked to the sensitivity of Asf1 mutants to DNA-damaging agents (methyl methane sulfonate [MMS]) and replication stress (hydroxyurea [HU]) (Ramey et al., 2004). None of the single mutations in Asf1 led to pronounced defects in growth (Table 1). However, L6M, S48R, V109M, Y112A, V146L, and T147E led to enhanced transcriptional silencing of an *HMR::ADE2* reporter (apparent from the red colonies in Figures 5A and S3), as compared to the normal Asf1 protein. Additionally, these mutants had enhanced telomeric silencing of a *TELVIIL::URA3* reporter, as indicated by their increased ability to grow on 5′-fluoroorotic acid (5′-FOA) (Figure 5A, data not shown).

We also conducted phenotypic analysis with pairs of Asf1 mutations. T147E/R145E, Y112A/T147E, and Y112A/R145E had a growth defect similar to that of yeast-lacking Asf1 (*asf1Δ*), as revealed by the small colony size on rich media (Figures 5B and 5C). Consistent with their growth defect, we found that the pairs of Asf1 mutations T147E/R145E, Y112A/T147E, and Y112A/R145E led to MMS and HU sensitivity that was similar to *asf1Δ* (Figure 5B). The ability of the Asf1 T147E/R145E, Y112A/T147E, and Y112A/R145E proteins to mediate transcriptional silencing of the *HMR::ADE2* reporter was also indistinguishable from *asf1Δ*, as these strains yielded white colonies (Figure 5C). The R145E/S48R mutant of Asf1 had intermediate activity, producing yeast colonies that were smaller than wild-type, being sensitive to elevated concentrations of MMS and HU and having a silencing defect (Figures 5B and 5C).

To determine the role of the interactions between Asf1 and histones H3/H4 in chromatin disassembly, we measured the ability of *asf1* mutants to activate the *PHO5* gene. Asf1-mediated chromatin disassembly of the *PHO5* gene promoter is required for transcriptional activation (Adkins et al., 2004). Asf1 mutations that inactivate Asf1 function in all the assays shown above, i.e., V94R, Y112A/R145E, Y112A/T147E, and T147E/R145E, completely failed to activate the *PHO5* gene, indicating that these mutations also disrupt the chromatin-disassembly activity of Asf1 (Figure 5D). S48R resembled wild-type Asf1 for *PHO5* activation, V109M was slightly defective at activating *PHO5*, and V146L had a more significant defect in *PHO5* activation (Figure 5D).

To ascertain whether the mutations alter the binding of Asf1 to histones H3/H4, we examined their effects on the Asf1-H3/H4 complex in vivo and in vitro. All of the Asf1 mutations prevented our ability to detect coimmunoprecipitating histones from yeast (Figure 5E). Similarly, in the reciprocal immunoprecipitation analysis, all the mutations prevented our ability to detect Asf1 coimmunoprecipitating with histone H4 (Figure 5E). We further tested the effect of the Asf1 mutations on the ability to purify the recombinant Asf1-H3/H4 complex from *E. coli*. At similar loadings of GST-Asf1 onto the glutathione-affinity resin, all the Asf1 mutants that were examined had greatly reduced amounts of copurifying H3/H4 when compared to wild-type Asf1 (Figure 5F). In particular, the binding of Asf1 mutants S48R, Y112A, and S48R/R145E to H3/H4 was drastically reduced to levels equivalent to the V94R disruptive mutation of Asf1, as was the binding of T147E, R145E, and Y112A/T147E (data not shown). Asf1 mutations V109M and V146L also showed significantly reduced binding to H3/H4. Asf1 T147E/R145E had the greatest reduction in H3/H4 binding seen for any Asf1 mutant to date. As such, the mutations in Asf1 that were designed to decrease histone H3/H4 binding (Figure 5G) do indeed weaken the Asf1-histone H3/H4 interaction.

## Disruption of Asf1 Function by Mutations in the Asf1 Binding Interfaces of Histones H3/H4

In order to further examine the physiological relevance of the interaction between Asf1 and histone H4, we created mutations in the region of H4 predicted to alter the Asf1-H4 interaction. Amino acids 92–102 were deleted from H4 in order to eliminate binding of H4 to Asf1. H4 Δ92–102

**Table 1. Summary of Phenotypes of Asf1, H3, and H4 Mutants in the Interaction Interface**

| | Growth | Silencing | MMS Resistance | HU Resistance | Zeocin Resistance | *PHO5* Induction |
|---|---|---|---|---|---|---|
| ASF1 WT | +++ | + | ++ | ++ | +++ | ++++ |
| asf1Δ | + | - | - | - | + | - |
| **Asf1 mutants:** | | | | | | |
| T147E | +++ | ++ | nd | nd | +++ | nd |
| R145E | +++ | +/− | nd | nd | +++ | nd |
| L6M | +++ | ++ | nd | nd | +++ | nd |
| V109M | +++ | ++ | ++ | ++ | +++ | +++ |
| V146L | +++ | ++ | ++ | ++ | +++ | ++ |
| P144Y | +++ | + | nd | nd | +++ | nd |
| Y112A | +++ | ++ | nd | nd | +++ | nd |
| S48R | +++ | ++ | ++ | ++ | +++ | ++++ |
| V94R | + | - | - | - | +++ | - |
| Y162A | +++ | + | nd | nd | +++ | nd |
| T147E/R145E | + | +/− | - | - | +++ | - |
| Y112A/R145E | + | - | - | - | +++ | - |
| Y112A/P144Y | +++ | + | ++ | ++ | +++ | nd |
| Y112A/T147E | + | - | - | - | + | - |
| Y112A/V146L | +++ | + | ++ | ++ | +++ | nd |
| S48R/T147E | +++ | + | ++ | ++ | +++ | nd |
| S48R/R145E | ++ | - | + | + | +++ | + |
| S48R/P144Y | +++ | ++ | nd | nd | nd | nd |
| **H4 mutants:** | | | | | | |
| F100A | +++ | - | ++ | + | +++ | +++ |
| R92A[1] | +++ | +* | ++ | ++ | - | ++ |
| H75Y[2] | +++ | ++* | ++ | ++ | + | +++ |
| Δ92-102 | - | n/a | n/a | n/a | n/a | n/a |
| Y72G[3] | + | nd | ++ | + | + | +++ |
| Y88G[3] | ++ | nd | ++ | + | - | ++++ |
| **H3 mutants:** | | | | | | |
| K122Q[2] | +++ | -* | ++ | ++ | - | ++++ |
| K115A[2] | +++ | +* | ++ | + | - | ++ |
| K122A[2] | +++ | -* | ++ | ++ | - | ++ |

The indicated mutants were previously described in the following papers: [1](Hyland et al., 2005), [2](Xu et al., 2005), and [3](Santisteban et al., 1997). The phenotypes designated with * indicate phenotypes determined from these previous publications. n/a = not applicable, nd = not determined.

was found to be inviable as the sole source of histone H4 in the cell (Table 1), indicating that the C terminus of histone H4 may perform an important role in the structure of the nucleosome per se. Additionally, F100A was created to alter the contacts between H4 and the pocket of Asf1 (Figures 4B and 4C). The F100A mutation caused no significant growth defect (Table 1), indicating that H4 F100 does not mediate critical contacts within the nucleosome. However, H4 F100A caused slight sensitivity to replication stress (Figure 6A) and led to a defect in transcriptional silencing comparable to deletion of the *ASF1* gene (Figure S4). The H4 F100A mutation also led to a reduced ability to disassemble chromatin from the *PHO5* promoter (Figure 6B), indicating a role for the Asf1-H4 F100 interaction in chromatin disassembly. When we examined the effect of these H4 mutations on the ability of H3/H4 to

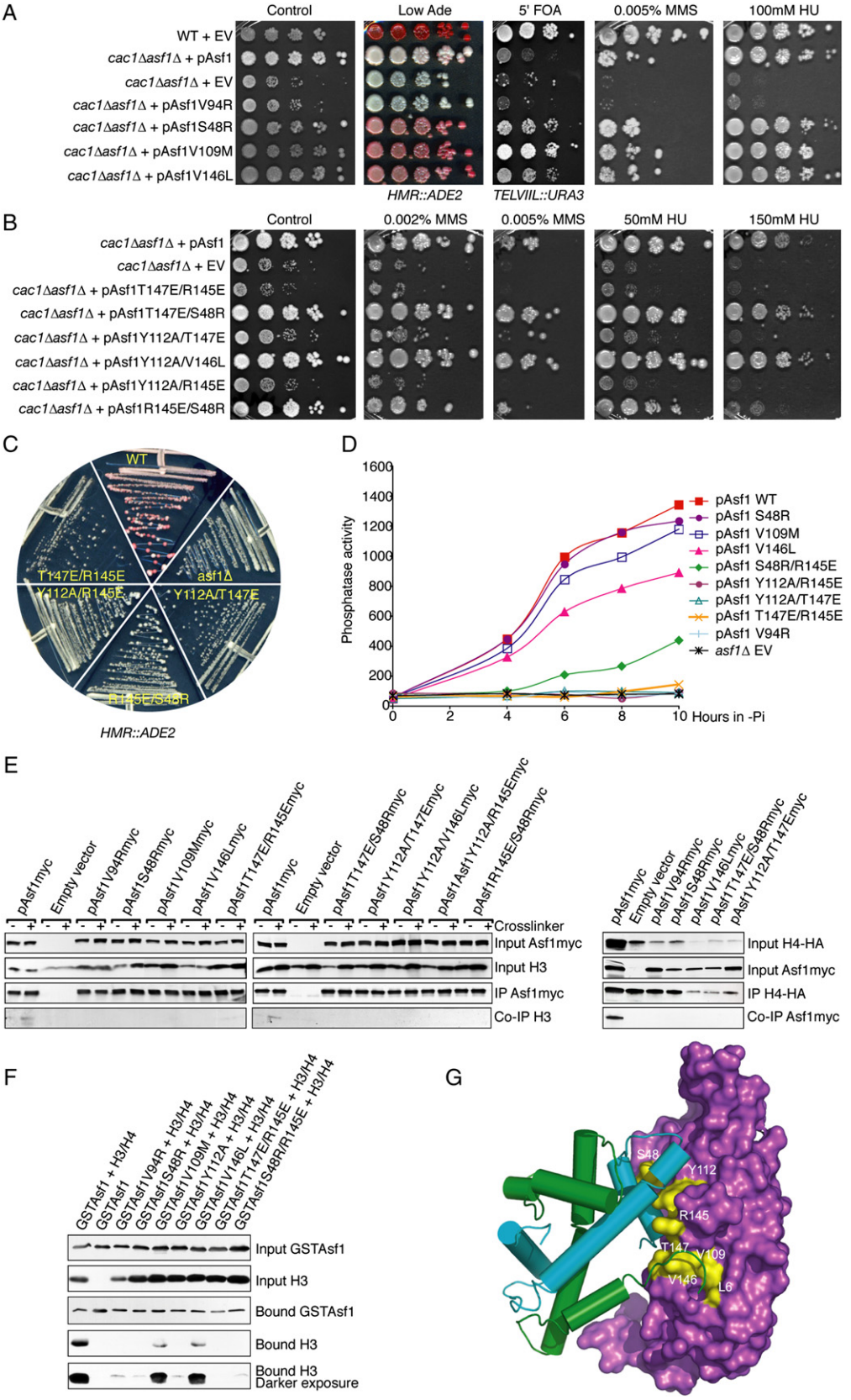
A
Control
Low Ade
5' FOA
0.005% MMS
100mM HU
WT + EV
cac1Δasf1Δ + pAsf1
cac1Δasf1Δ + EV
cac1Δasf1Δ + pAsf1V94R
cac1Δasf1Δ + pAsf1S48R
cac1Δasf1Δ + pAsf1V109M
cac1Δasf1Δ + pAsf1V146L
HMR::ADE2
TELVIIL::URA3
B
Control
0.002% MMS
0.005% MMS
50mM HU
150mM HU
cac1Δasf1Δ + pAsf1
cac1Δasf1Δ + EV
cac1Δasf1Δ + pAsf1T147E/R145E
cac1Δasf1Δ + pAsf1T147E/S48R
cac1Δasf1Δ + pAsf1Y112A/T147E
cac1Δasf1Δ + pAsf1Y112A/V146L
cac1Δasf1Δ + pAsf1Y112A/R145E
cac1Δasf1Δ + pAsf1R145E/S48R
C
WT
T147E/R145E
Y112A/R145E
asf1Δ
Y112A/T147E
R145E/S48R
HMR::ADE2
D
Phosphatase activity
Hours in -Pi
pAsf1 WT
pAsf1 S48R
pAsf1 V109M
pAsf1 V146L
pAsf1 S48R/R145E
pAsf1 Y112A/R145E
pAsf1 Y112A/T147E
pAsf1 T147E/R145E
pAsf1 V94R
asf1Δ EV
E
pAsf1myc
Empty vector
pAsf1V94Rmyc
pAsf1S48Rmyc
pAsf1V109Mmyc
pAsf1V146Lmyc
pAsf1T147E/R145Emyc
pAsf1T147E/S48Rmyc
pAsf1Y112A/T147Emyc
pAsf1Y112A/V146Lmyc
pAsf1Asf1Y112A/R145Emyc
pAsf1R145E/S48Rmyc
pAsf1V146Lmyc
pAsf1T147E/S48Rmyc
Crosslinker
Input Asf1myc
Input H3
IP Asf1myc
Co-IP H3
Input H4-HA
Input Asf1myc
IP H4-HA
Co-IP Asf1myc
F
GSTAsf1 + H3/H4
GSTAsf1
GSTAsf1V94R + H3/H4
GSTAsf1S48R + H3/H4
GSTAsf1V109M + H3/H4
GSTAsf1Y112A + H3/H4
GSTAsf1V146L + H3/H4
GSTAsf1T147E/R145E + H3/H4
GSTAsf1S48R/R145E + H3/H4
Input GSTAsf1
Input H3
Bound GSTAsf1
Bound H3
Bound H3
Darker exposure
G
S48
Y112
R145
T147
V109
V146
L6

copurify with GSTAsf1 from *E. coli*, we observed a defect resulting from the F100A mutation (Figure 6C). H4 Δ94–102 also greatly reduced the ability of H3/H4 to copurify with Asf1. As such, the C terminus of H4 plays an important role in the interaction of Asf1 with H3/H4 and the function of Asf1 in vivo.

We also analyzed other mutations in histone H4, H75Y, R92A, Y88G, and Y72G, which were expected to weaken the binding of H4 to Asf1 (Hyland et al., 2005; Santisteban et al., 1997; Xu et al., 2005) (Figure 3B). We found that the growth defects caused by H4 Y72G and Y88G (Santisteban et al., 1997) were similar to that of yeast deleted for *ASF1* (Figure S5). The most pronounced effect of these H4 mutations was their sensitivity to the radiomimetic Zeocin that results in double-strand DNA breaks (Figure 6A). In order to examine the ability of these H4 mutants to disassemble chromatin, they were compared to their isogenic wild-type strains for their ability to activate *PHO5*. We found that H4 R92A had a strong defect in *PHO5* activation, while H4 H75Y and H4 Y72G had minor defects in *PHO5* activation (Figure 6B, Table 1). Taken together, these results demonstrate that four mutations in histone H4 in the region that binds to Asf1 (Figure 6D) reduce the ability of Asf1 to mediate chromatin disassembly, indicating the importance of the Asf1-H4 interaction in chromatin disassembly.

To further characterize the physiological relevance of the interactions between Asf1 and histone H3, we examined available mutations in regions of histone H3 (Hyland et al., 2005; Santisteban et al., 1997; Xu et al., 2005) that we predicted would weaken the interaction with Asf1 (Figure 2B). We found that H3 K115A led to sensitivity to HU to the same extent as deletion of *ASF1*, whereas K115A, K122A, and K122Q led to sensitivity to Zeocin that was even more pronounced than that resulting from deletion of *ASF1* (Figure 6A). Furthermore, we found that K115A and K122A but not K122Q led to a defect in Asf1-mediated chromatin disassembly (Figure 6B). Importantly, the altered activity of the histone mutants was not due to potential differences in protein stability, as the mutants were all expressed to the same level as wild-type histones (Figure S6). These results indicate that the interaction between Asf1 and histone H3 contributes to the function of Asf1 during DNA replication and DNA repair (presumably in chromatin assembly) and to chromatin disassembly during transcriptional activation.

## DISCUSSION

Here we present the only structure to date of a histone chaperone bound to histones. The structure of Asf1 bound to a heterodimer of H3/H4 was confirmed to be the physiologically relevant form of the Asf1-H3/H4 complex by extensive mutagenesis analyses in yeast and in vitro. This complex reveals the altered conformations of the histones outside of the nucleosome. Although the Asf1 structure was not drastically altered by binding to the histones, larger conformational changes occurred in both histones H3 and H4 in the Asf1 complex, as compared to their structures within the nucleosome. Remarkably, there was a dramatic change in the conformation of the C-terminal tail of H4 upon binding to Asf1 through β strand addition (Figures 4D–4F).

### Functional Investigation of the Asf1-H3/H4 Interactions

The ubiquitous function of Asf1 in eukaryotes is highlighted by the sequence conservation of the residues involved in the interactions between Asf1 and histones H3/H4 (Figures S1 and S7). Budding yeast Asf1 is 56% identical to *Xenopus* Asf1 in the conserved core, and the *Xenopus* histones are 88% and 92% identical to H3 and H4 from yeast, respectively (Figure S1). Only the following three residues of *Xenopus* H3 that contact Asf1 differ in other species: C110 (Ala in yH3), Q125 (Lys in yH3), and I130 (Leu in yH3); these substitutions would appear to cause only minor and possibly compensated differences in interprotein packing. Furthermore, none of these interspecies differences occur in residues of H4 that contact Asf1. Therefore, the interactions observed in this structure will likely be applicable to Asf1-histone H3/H4 complexes from different species.

The Asf1 histone chaperone forms extensive contacts with both histones H3 and H4. The Asf1-H3/H4 structure reveals the details of the interface between Asf1 and α3 of H3 and has identified a new interaction between Asf1

**Figure 5. Disruption of Asf1 Functions by Mutations in the Histone Binding Interfaces**

(A) Asf1 mutations that lead to enhanced transcriptional silencing. A wild type (WT) strain containing pRS314 (EV) and *cac1Δasf1Δ* containing pRS314 (EV) or the wild type or mutagenized pAsf1 plasmid (as indicated) were analyzed by 10-fold serial-dilution analysis onto the indicated plates.

(B) Asf1 mutations that inactivate Asf1. *cac1Δasf1Δ* containing pRS314 (EV), pAsf1 plasmid, or mutagenized pAsf1 (as indicated) were analyzed as in A.

(C) Analyses of growth and silencing in Asf1 mutants.

(D) Ability of *asf1* mutants to activate the *PHO5* gene. Phosphate was depleted from the media of strains *cac1Δasf1Δ* carrying the indicated plasmids at time 0, and samples were taken and assayed for acid phosphatase activity.

(E) Disruption of the Asf1-histone interaction by Asf1 mutations in yeast. Coimmunoprecipitation analysis (left panel) was performed using an anti-myc antisera from strain ROY1169 carrying the indicated plasmids. The inclusion of the DSP crosslinker is indicated by the plus (+) sign. The input and immunoprecipitation (IP) samples were western blotted as indicated. Coimmunoprecipitation analysis (right panel) was performed using anti-HA antisera from strain ROY1169 carrying the indicated plasmids and overexpressing HA-H4.

(F) Disruption of the Asf1-histone interaction by Asf1 mutations in vitro. The inputs of the indicated coexpressed proteins and the material bound to the glutathione affinity column were western blotted as indicated.

(G) Locations of the Asf1 substitutions that alter Asf1 function.

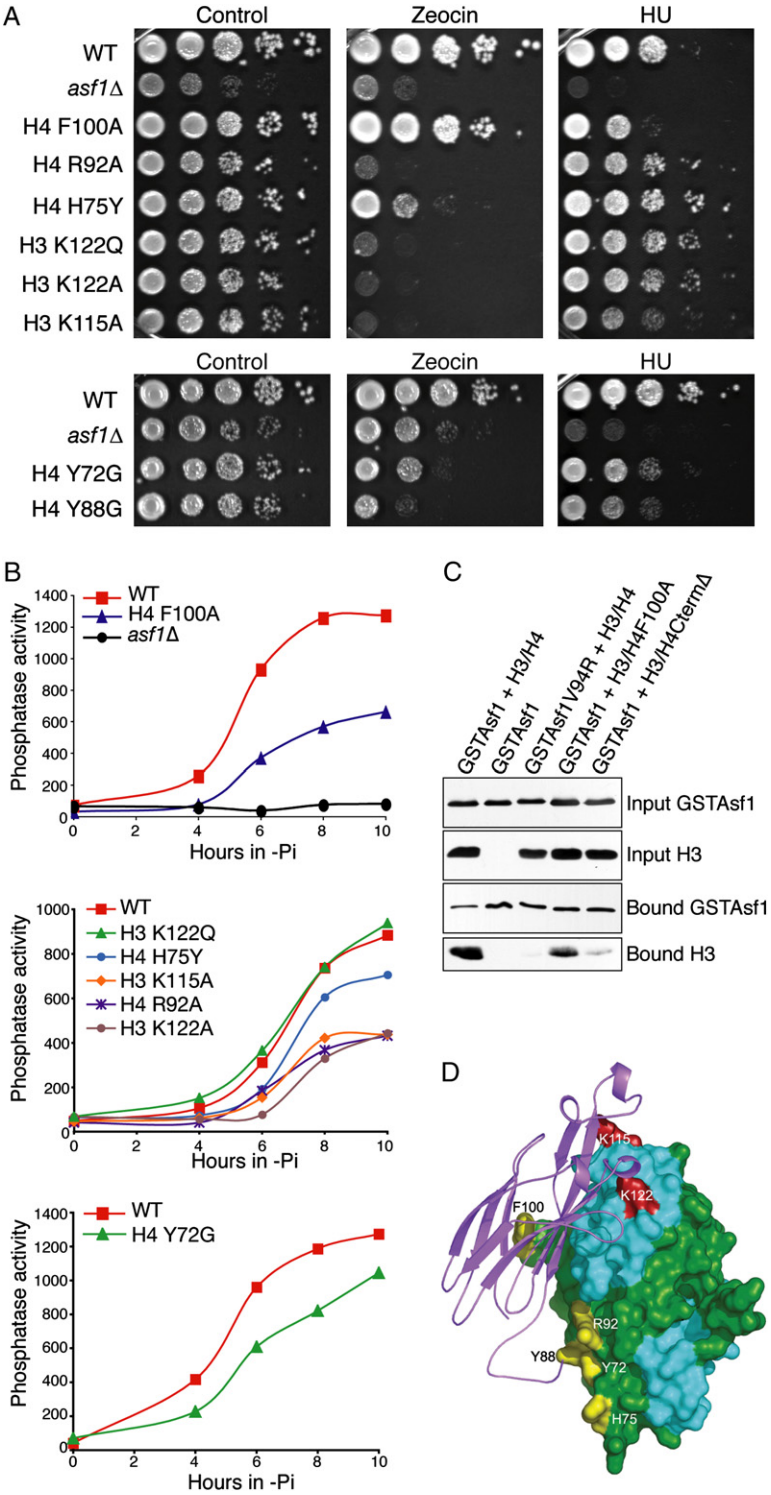


**Figure 6. Disruption of Asf1 Functions by Mutations of H3/H4**

(A) Sensitivity of histone mutants to DNA damaging agents and replication stress, as described in Figure 5A.

(B) Phosphatase activity was measured as described in Figure 5D.

(C) The stability of the Asf1-H3/H4 complex is reduced by the F100A mutation or deletion of residues 92-102 of histone H4. The analysis was performed as described in Figure 5F.

(D) Location of the H3 (in red) and H4 residues (in yellow) whose mutation alters Asf1 function.

and α2 of H3. The implications of the mutagenesis study, with regard to Asf1 and H3, are that disruption of this intricate interface has severe consequences in the context of the cellular activity. For example, mutations in the regions of Asf1 that bind to only H3 (R145E/S48R, Y112A/R145E, V94R, and S48R) or the region of H3 that binds to Asf1 (K115 and K122) weakened the interaction between Asf1 and H3 and disrupted Asf1 function in vivo and in vitro (Figures 5 and 6). As such, the interaction between histone H3 and Asf1 is clearly critical for its cellular functions.

The Asf1-H3/H4 structure shows extensive contacts between Asf1 and histone H4 (Figure 3). This interface has two parts: (1) the globular core of Asf1 interacts with the C-terminal tail of H4 to form a strand-swapped dimer and (2) the C-terminal tail of Asf1 binds to the histone-fold region (α3) of histone H4. These interactions are also important because mutations in residues of Asf1 that contact H4 (T147, L6, V109, and V146) weaken histone binding (Figures 5E and 5F) and alter the functions of Asf1 in yeast (Figure 5, Table 1) (Recht et al., 2006). Similarly, mutation of histone H4 residues R92, H75, Y72, Y88, and F100 that contact Asf1 in the Asf1-H3/H4 structure reduces the chromatin assembly and/or disassembly functions of Asf1 in vivo (Figure 6). Clearly, interactions of Asf1 with both histones H3 and H4 are required for Asf1 function, and neither interaction is sufficient.

The mutations that affect the interaction between Asf1 and H3/H4 fall into two distinct functional classes; (1) those that reduce the function of Asf1 and (2) those that cause a gain-of-function phenotype. The former was expected, but the latter uncovered specific mutations that overcome the requirement for CAF-1 in transcriptional silencing. These include Asf1 S48R, V109M, Y112E, and V146L that weaken the interaction with histones H3/H4 in vivo and in vitro. Interestingly, the histone H4 H75Y mutation that had reduced Asf1-mediated chromatin-disassembly activity and Zeocin sensitivity (Figure 6) has also been previously shown to bypass the requirement for CAF-1 in silencing (Xu et al., 2005). We recently observed the same ability to bypass the requirement for CAF-1 in silencing by truncations or insertion mutations in the C terminus of Asf1 (Tamburini et al., 2006). Specifically, we found that inactivation of CAF-1 led to reduced histone deposition onto DNA, while additional mutations in the C terminus of Asf1 restored the histone deposition onto DNA (Tamburini et al., 2006). Although the C terminus of Asf1 is not present in our structure, it may extend toward histone H4 from its current location in the structure and may contribute further to histone binding affinity. It is possible that the Asf1 L6M, S48R, V109M, Y112E, V146L, and T147E mutations enhance transcriptional silencing by the same mechanism as the C-terminal mutations in Asf1.

## Implications for Function of Other Histone Chaperones

Histone chaperones exhibit common structural features that suggest a similar mode of histone binding. For example, a variant of the anti-parallel β sheet region of Asf1, which interacts with histones H3 and H4 in the Asf1-H3/H4 structure, is also found in Nap1 and all histone chaperone structures (Park and Luger, 2006), including nucleoplasmin (Np and nucleoplasmin-like proteins) (Namboodiri et al., 2003, 2004). Interestingly, the RbAp48 and p60 subunits of CAF-1 (Kaufman et al., 1995; Verreault et al., 1996) and the histone-chaperone HIRA (Desilva et al., 1998) are composed of WD-40 repeats that are predicted to adopt β-propeller structures with exposed β sheets. In the Asf1-H3/H4 structure, an acidic face of this conserved β sheet in Asf1 forms the platform for interaction of H3 and may also contribute to orientation of the complex through electrostatic steering. Thus, for the other histone chaperones, it is possible that α3 of H2B or H3 (or another region of the histone dimer) also binds to the acidic and exposed face of these β sheets.

A prominent general feature of the histone-chaperone structures is the exposure of the edges of β sheets in these proteins (Park and Luger, 2006). One exposed β sheet edge of Asf1 forms the site for β strand addition by the C terminus βC of H4 (Figure 3B). Exposure of the edges of β sheets occurs either as part of a β sheet sandwich (Asf1), a double pentamer of β sheet sandwiches (Np, Nlp, and NO38) (Namboodiri et al., 2003, 2004), or as a single sheet with at least one edge exposed (Nap1 and WD-40 repeat proteins) (Park and Luger, 2006). Interestingly, both histones H4 and H2A also have the propensity for β strand formation in their C termini (Luger et al., 1997). In the structure of Np there is acidic character to the exposed β sheet, which is a favorable site for β-strand addition by either H4 or H2A, particularly with the βH domain or the β1 strand of Np (Namboodiri et al., 2003). There is also a hydrophobic pocket in the neighboring Np monomer, which contains several well-conserved residues (F30, L47, L45, I94, W19, and F102) and resembles the hydrophobic pocket where H4 inserts into Asf1. As such, our structure provides a framework for understanding a possible mode in which other histones chaperones may bind to histones.

## Implications for the Assembly of Chromatin

The Asf1-H3/H4 structure clearly demonstrates that Asf1 escorts H3/H4 histones as a heterodimer, rather than the heterotetramer that is seen in the nucleosome. It has been a widely held belief that soluble histones H3 and H4 exist as H3/H4 heterotetramers in the cell because extraction of histones from cells yielded H3/H4 in a heterotetrameric form (Moss et al., 1976). The Asf1-H3/H4 structure shows that Asf1 binds to an H3/H4 heterodimer, physically blocking formation of the H3/H4 heterotetramer by enveloping precisely the same residues of H3 that are involved in the formation of the four-helix bundle formed by the H3:H3 dimer in the nucleosome (Luger et al., 1997). This discovery raises the question of whether the H3/H4 heterotetramer is assembled from two H3/H4 heterodimers prior to deposition onto the DNA or whether two H3/H4 heterodimers are deposited sequentially or concertedly onto DNA, and the possibility that other H3/H4 chaperones may assist Asf1 in the transfer of the H3/H4 dimer or tetramer to DNA. Clearly, the mechanism of formation of the H3/H4 heterotetramer on DNA must involve removal of Asf1 from histone H3 to enable H3:H3 dimerization. The trigger for removal of Asf1 from histone H3 is unknown, but it may be the presence of DNA, as the addition of DNA to histone bound Asf1 results in chromatin assembly in vitro (English et al., 2005; Krawitz et al., 2002). However, the specific role of Asf1-DNA interactions during this process is unclear (Padmanabhan et al., 2005).

As such, the mechanism of how chromatin is assembled and disassembled needs to be further investigated.

## A Proposed Mechanism for the Disassembly of Nucleosomes

A key feature of the novel interaction between Asf1 and histone H4 is the formation of the strand-swapped anti-parallel β sheet, which is a unique conformation not seen for H4 in any nucleosome or octamer structures. The C terminus of H4 normally forms a parallel β sheet with histone H2A in the nucleosome (Luger et al., 1997) that stabilizes the interaction between the H3/H4 heterotetramer and H2A/H2B heterodimers within the nucleosome. However, in the Asf1-H3/H4 complex, the H4 C terminus rotates almost 180° to form an anti-parallel β sheet with strand β9 of Asf1 (Figure 4). This raises the intriguing possibility that the C terminus of H4 can act as a handle for chromatin disassembly.

In this "strand-capture" model for disassembly of histone H3/H4 tetramers, Asf1 captures the C terminus of H4 and uses it to aid in formation of the Asf1-H3/H4 complex. This interaction could potentially occur even when H4 is sequestered in the H3/H4 heterotetramer. Therefore, Asf1 binding to the C terminus of H4 may be the first step and the trigger for splitting the H3/H4 heterotetramer into Asf1 bound H3/H4 heterodimers during chromatin disassembly. The molecular mechanism of the strand-capture model could be either that Asf1 alone or together with another remodeling activity uses the H4 C terminus as a lever to unzip the H3/H4 heterotetramer, or that the association of Asf1 with the C terminus of H4 could tether Asf1 so that binding to the H3 dimerization interface could occur more readily. The model also suggests that the formation of a new β strand in the H4 C terminus and the lock-and key binding observed for F100 of H4, that fits snugly into the pocket on the surface of Asf1, would provide sufficient binding energy to sequester the H3/H4 tetramer, but this binding affinity is currently unknown (Figure 4B).

This strand capture model is supported by the in vivo and in vitro data. Disruption of the interaction of the H4 C-terminal tail with both the binding pocket of the Asf1 core and with the C-terminal region of Asf1 led to defects in chromatin disassembly and transcriptional silencing and deficiencies in Asf1-H3/H4 complex formation in vivo and in vitro (Figures 5 and 6). Indeed, the involvement of H4 F100 and the Asf1 pocket in chromatin disassembly is seen by the defects in *PHO5* gene activation resulting from substitutions H4 F100A, Asf1 V109M, and Asf1 V146L that disrupt this interaction (Figures 3C, 5, and 6). A feature of this chromatin disassembly model is that Asf1 can only access the C-terminal tail of H4 once the H2A/H2B dimers are removed, potentially by other histone chaperones. This model is in accord with recent studies that Asf1 alone cannot mediate histone disassembly from nucleosomes in vitro (Lorch et al., 2006), suggesting that an H2A/H2B chaperone is necessary to remove H2A/H2B first. Furthermore, the C-terminal tail of H4 in the nucleosome would not be fully accessible to Asf1 without unwinding the outermost gyre of the DNA, indicating that an ATP-dependent chromatin-remodeling activity may be required prior to or concomitant with Asf1-mediated removal of H3/H4 from the DNA.

## Conclusions

Characterization of the Asf1-H3/H4 complex provides the basis for interpretation of a wealth of functional and structural studies. The structure is consistent with all of the biological data and mutagenesis analyses on Asf1 and histones to date. In addition to providing novel insights into the structure of histone chaperones bound to histones, this work gives insights into new potential mechanisms of nucleosome assembly and disassembly. Furthermore, it poses hypotheses about histone-carrying mechanisms that may be generally applicable to other histone-chaperone proteins.

## EXPERIMENTAL PROCEDURES

### Crystallization, Structure Determination, and Analysis

The mutant and wild-type Asf1-H3/H4 complexes were coexpressed and purified as described in English et al. (2005). Crystallization conditions were identified using the Fluidigm system (Hansen and Quake, 2003). Data from crystals (space group $P3_121$; cell dimensions, a = b = 95.75 Å, c = 110.68 Å) were collected on beamline 4.4.2 at the Advanced Light Source (Berkeley, CA) and were processed using D*Trek (Pflugrath, 1999). The structure was solved by molecular replacement using Phaser (McCoy et al., 2005) and refined using Refmac (CCP4) (Bailey, 1994) and O (Kleywegt and Jones, 1996) (Table 1). The model contains residues 1–164 of Asf1 (chain A), 60–134 of H3 (chain B), and 20–101 of H4 (chain C), and the side chains of H3 Y98, K133, and Asf1 N156 were built as alanine. Structural analyses used CCP4, Superpose (Maiti et al., 2004), and LSQMAN (Kleywegt, 1996) programs, and structure diagrams were made using MOLSCRIPT (Kraulis, 1991), VMD (Humphrey et al., 1996), and PyMOL (DeLano, 2002).

### Yeast Analyses

Yeast strains and plasmids are described in the Supplemental Data. Resistance to methyl methane sulfonate (MMS), Zeocin, and hydroxyurea (HU) was determined by 10-fold dilution analysis of 1 OD 600 nm logarithmically growing cultures of yeast strains onto plates containing the indicated amount of the agents. Transcriptional silencing of the *TELVIIL::URA3* and the *HMR::ADE2* reporters was measured by plating onto 1 mg/ml 5′-FOA and onto low adenine plates respectively. The ability to activate the *PHO5* gene was measured as previously described, as an indicator of Asf1-mediated promoter chromatin disassembly (Adkins et al., 2004). Coimmunoprecipitation analysis of Asf1 and histones was performed as described previously (Tamburini et al., 2005).

### Supplemental Data

Supplemental Data include seven figures, three tables, experimental procedures, and references and can be found with this article online at http://www.cell.com/cgi/content/full/127/3/495/DC1/.

## ACKNOWLEDGMENTS

We thank members of the Tyler and Churchill labs, Leslie Krushel, Rui Zhao, and Jeff Kieft for critical reading of the manuscript. We are very grateful to Karolin Luger for histone plasmid constructs and advice. We thank Jeff Boeke, Jim Broach, and Mitch Smith for yeast strains, and Rui Zhao, Jeff Kieft, Jill Waters, and Sarah Roemer for technical support and advice. We thank Jay Nix and the staff at beamline 4.2.2 at

the Advanced Light Source, Lawrence Berkeley National Lab. The UCDHSC Biomolecular X-ray Crystallography Center was supported in part by funding from the HHMI, the UC Cancer Center, and NIH. This work was supported by NIH grant GM064475 (to J.K.T.) and by AHA grant 0355468Z (to M.E.A.C.). J.K.T. is a Leukemia and Lymphoma Society Scholar.

Received: May 13, 2006
Revised: July 28, 2006
Accepted: August 21, 2006
Published: November 2, 2006

## REFERENCES

Adkins, M.W., Howar, S.R., and Tyler, J.K. (2004). Chromatin disassembly mediated by the histone chaperone Asf1 is essential for transcriptional activation of the yeast PHO5 and PHO8 genes. Mol. Cell *14*, 657–666.

Akey, C.W., and Luger, K. (2003). Histone chaperones and nucleosome assembly. Curr. Opin. Struct. Biol. *13*, 6–14.

Arents, G., Burlingame, R.W., Wang, B.C., Love, W.E., and Moudrianakis, E.N. (1991). The nucleosomal core histone octamer at 3.1 Å resolution: a tripartite protein assembly and a left-handed superhelix. Proc. Natl. Acad. Sci. USA *88*, 10148–10152.

Bailey, S. (1994). The CCP4 suite: programs for protein crystallography. Acta Crystallogr. *D50*, 760–763.

Daganzo, S.M., Erzberger, J.P., Lam, W.M., Skordalakes, E., Zhang, R., Franco, A.A., Brill, S.J., Adams, P.D., Berger, J.M., and Kaufman, P.D. (2003). Structure and function of the conserved core of histone deposition protein Asf1. Curr. Biol. *13*, 2148–2158.

Davey, C.A., Sargent, D.F., Luger, K., Maeder, A.W., and Richmond, T.J. (2002). Solvent mediated interactions in the structure of the nucleosome core particle at 1.9 Å resolution. J. Mol. Biol. *319*, 1097–1113.

DeLano, W.L. (2002). The PyMOL Molecular Graphics System (San Carlos, CA: DeLano Scientific).

Desilva, H., Lee, K., and Osley, M.A. (1998). Functional dissection of yeast Hir1p, a WD repeat-containing transcriptional corepressor. Genetics *148*, 657–667.

English, C.M., Maluf, N.K., Tripet, B., Churchill, M.E., and Tyler, J.K. (2005). ASF1 binds to a heterodimer of histones H3 and H4: A two-step mechanism for the assembly of the H3-H4 heterotetramer on DNA. Biochemistry *44*, 13673–13682.

Green, E.M., Antczak, A.J., Bailey, A.O., Franco, A.A., Wu, K.J., Yates, J.R., 3rd, and Kaufman, P.D. (2005). Replication-independent histone deposition by the HIR complex and Asf1. Curr. Biol. *15*, 2044–2049.

Groth, A., Ray-Gallet, D., Quivy, J.P., Lukas, J., Bartek, J., and Almouzni, G. (2005). Human Asf1 regulates the flow of S phase histones during replicational stress. Mol. Cell *17*, 301–311.

Hansen, C., and Quake, S.R. (2003). Microfluidics in structural biology: smaller, faster… better. Curr. Opin. Struct. Biol. *13*, 538–544.

Humphrey, W., Dalke, A., and Schulten, K. (1996). VMD: Visual molecular dynamics. J. Mol. Graph. *14*, 33–38, 27–28.

Hyland, E.M., Cosgrove, M.S., Molina, H., Wang, D., Pandey, A., Cottee, R.J., and Boeke, J.D. (2005). Insights into the role of histone H3 and histone H4 core modifiable residues in *Saccharomyces cerevisiae*. Mol. Cell. Biol. *25*, 10060–10070.

Kaufman, P.D., Kobayashi, R., Kessler, N., and Stillman, B. (1995). The p150 and p60 subunits of chromatin assembly factor I: a molecular link between newly synthesized histones and DNA replication. Cell *81*, 1105–1114.

Kleywegt, G.J. (1996). Use of non-crystallographic symmetry in protein structure refinement. Acta Crystallogr. *D52*, 842–857.

Kleywegt, G.J., and Jones, T.A. (1996). Efficient rebuilding of protein structures. Acta Crystallogr. *D52*, 829–832.

Kraulis, P.J. (1991). Molscript - a program to produce both detailed and schematic plots of protein structures. J. Appl. Crystallogr. *24*, 946–950.

Krawitz, D.C., Kama, T., and Kaufman, P.D. (2002). Chromatin assembly factor I mutants defective for PCNA binding require Asf1/Hir proteins for silencing. Mol. Cell. Biol. *22*, 614–625.

Lorch, Y., Maier-Davis, B., and Kornberg, R.D. (2006). Chromatin remodeling by nucleosome disassembly in vitro. Proc. Natl. Acad. Sci. USA *103*, 3090–3093.

Loyola, A., and Almouzni, G. (2004). Histone chaperones, a supporting role in the limelight. Biochim. Biophys. Acta *1677*, 3–11.

Luger, K. (2003). Structure and dynamic behavior of nucleosomes. Curr. Opin. Genet. Dev. *13*, 127–135.

Luger, K., Mader, A.W., Richmond, R.K., Sargent, D.F., and Richmond, T.J. (1997). Crystal structure of the nucleosome core particle at 2.8 Å resolution. Nature *389*, 251–260.

Maiti, R., Van Domselaar, G.H., Zhang, H., and Wishart, D.S. (2004). SuperPose: a simple server for sophisticated structural superposition. Nucleic Acids Res *32*, W590–W594.

McCoy, A.J., Grosse-Kunstleve, R.W., Storoni, L.C., and Read, R.J. (2005). Likelihood-enhanced fast translation functions. Acta Crystallogr. *D61*, 458–464.

Mello, J.A., Sillje, H.H., Roche, D.M., Kirschner, D.B., Nigg, E.A., and Almouzni, G. (2002). Human Asf1 and CAF-1 interact and synergize in a repair-coupled nucleosome assembly pathway. EMBO Rep. *3*, 329–334.

Moss, T., Cary, P.D., Crane-Robinson, C., and Bradbury, E.M. (1976). Physical studies on the H3/H4 histone tetramer. Biochemistry *15*, 2261–2267.

Mousson, F., Lautrette, A., Thuret, J.Y., Agez, M., Courbeyrette, R., Amigues, B., Becker, E., Neumann, J.M., Guerois, R., Mann, C., and Ochsenbein, F. (2005). Structural basis for the interaction of Asf1 with histone H3 and its functional implications. Proc. Natl. Acad. Sci. USA *102*, 5975–5980.

Munakata, T., Adachi, N., Yokoyama, N., Kuzuhara, T., and Horikoshi, M. (2000). A human homologue of yeast anti-silencing factor has histone chaperone activity. Genes Cells *5*, 221–233.

Nakatani, Y., Ray-Gallet, D., Quivy, J.P., Tagami, H., and Almouzni, G. (2004). Two distinct nucleosome assembly pathways: dependent or independent of DNA synthesis promoted by histone H3.1 and H3.3 complexes. Cold Spring Harb. Symp. Quant. Biol. *69*, 273–280.

Namboodiri, V.M.H., Dutta, S., Akey, I.V., Head, J.F., and Akey, C.W. (2003). The crystal structure of drosophila NLP-core provides insight into pentamer formation and histone binding. Structure *11*, 175–186.

Namboodiri, V.M.H., Akey, I.V., Schmidt-Zachmann, M.S., Head, J.F., and Akey, C.W. (2004). The structure and function of Xenopus NO38-core, a histone chaperone in the nucleolus. Structure *12*, 2149–2160.

Padmanabhan, B., Kataoka, K., Umehara, T., Adachi, N., Yokoyama, S., and Horikoshi, M. (2005). Structural similarity between histone chaperone Cia1p/Asf1p and DNA-binding protein NF-{kappa}B. J. Biochem. (Tokyo) *138*, 821–829.

Park, Y.J., and Luger, K. (2006). The structure of nucleosome assembly protein 1. Proc. Natl. Acad. Sci. USA *103*, 1248–1253.

Pflugrath, J.W. (1999). The finer things in X-ray diffraction data collection. Acta Crystallogr. *D55*, 1718–1725.

Ramey, C.J., Howar, S., Adkins, M., Linger, J., Spicer, J., and Tyler, J.K. (2004). Activation of the DNA damage checkpoint in yeast lacking the histone chaperone anti-silencing function 1. Mol. Cell. Biol. *24*, 10313–10327.

Recht, J., Tsubota, T., Tanny, J.C., Diaz, R.L., Berger, J.M., Zhang, X., Garcia, B.A., Shabanowitz, J., Burlingame, A.L., Hunt, D.F., et al. (2006). Histone chaperone Asf1 is required for histone H3 lysine 56 acetylation, a modification associated with S phase in mitosis and meiosis. Proc. Natl. Acad. Sci. USA *103*, 6988–6993.

Santisteban, M.S., Arents, G., Moudrianakis, E.N., and Smith, M.M. (1997). Histone octamer function in vivo: mutations in the dimer-tetramer interfaces disrupt both gene activation and repression. EMBO J. *16*, 2493–2506.

Schwabish, M.A., and Struhl, K. (2006). Asf1 mediates histone eviction and deposition during elongation by RNA polymerase II. Mol. Cell *22*, 415–422.

Smith, S., and Stillman, B. (1991). Stepwise assembly of chromatin during DNA replication in vitro. EMBO J. *10*, 971–980.

Tagami, H., Ray-Gallet, D., Almouzni, G., and Nakatani, Y. (2004). Histone H3.1 and H3.3 complexes mediate nucleosome assembly pathways dependent or independent of DNA synthesis. Cell *116*, 51–61.

Tamburini, B.A., Carson, J.J., Adkins, M.W., and Tyler, J.K. (2005). Functional conservation and specialization among Eukaryotic Antisilencing function 1 histone chaperones. Eukaryot. Cell *4*, 1583–1590.

Tamburini, B., Carson, J., Linger, J.G., and Tyler, J.K. (2006). Dominant mutants of the *Saccharomyces cereivisiae* ASF1 histone chaperone bypass CAF-1 mediated nucleosome assembly and Sir protein recruitment during transcriptional silencing. Genetics.

Tyler, J.K., Adams, C.R., Chen, S.R., Kobayashi, R., Kamakaka, R.T., and Kadonaga, J.T. (1999). The RCAF complex mediates chromatin assembly during DNA replication and repair. Nature *402*, 555–560.

Verreault, A., Kaufman, P.D., Kobayashi, R., and Stillman, B. (1996). Nucleosome assembly by a complex of CAF-1 and acetylated histones H3/H4. Cell *87*, 95–104.

White, C.L., Suto, R.K., and Luger, K. (2001). Structure of the yeast nucleosome core particle reveals fundamental changes in internucleosome interactions. EMBO J. *20*, 5207–5218.

Xu, E.Y., Bi, X., Holland, M.J., Gottschling, D.E., and Broach, J.R. (2005). Mutations in the nucleosome core enhance transcriptional silencing. Mol. Cell. Biol. *25*, 1846–1859.

## Accession Numbers

The coordinates have been deposited in the Protein Data Bank under code 1D 2hue.